12th International Symposium on Turbulence and Shear Flow Phenomena (TSFP12)
Osaka, Japan (Online), July 19-22, 2022

SYMMETRY-INDUCED HIGH-MOMENT TURBULENT SCALING LAWS OF A SPATIALLY EVOLVING TURBULENT ROUND JET

Cat Tuong Nguyen
Chair of Fluid Dynamics, Department of Mechanical Engineering
Technical University of Darmstadt
64287 Darmstadt, Germany
nguyen@fdy.tu-darmstadt.de

Martin Oberlack
Chair of Fluid Dynamics, Department of Mechanical Engineering
Technical University of Darmstadt
64287 Darmstadt, Germany
oberlack@fdy.tu-darmstadt.de

ABSTRACT

A direct numerical simulation (DNS) of a spatially evolving turbulent round jet has been conducted at $Re_0 = 3500$ in a very large box using a fully turbulent pipe flow as an inlet to analyze classical and new scaling laws from the near up to the far-field. The primary object of this study is to deepen our knowledge on turbulent jet flows employing the symmetry based turbulence theory using the multi-point moment equations (MPME). With the DNS data the scaling laws derived from Lie symmetry analysis are validated and extended up to statistical moments of arbitrary order n. Further investigations show that when fitting the instantaneous moments to a Gaussian function of the normalized radius r/z, the prefactors of the exponents show a linear behavior in n. This suggests the existence of an additional statistical symmetry which, if confirmed, can only be found in the MPME rather than in the Navier-Stokes equations.

Introduction

Until today only a few DNS have been conducted for studying the fundamentals of a spatially developing turbulent round jet. The earliest work using DNS was done by Boersma *et al.* (1998) where the research group studied the effect of inflow conditions on the self-similarity scaling up to $z/D = 45$ for a Reynolds number of $Re_0 = 2400$ based on the orifice diameter. In this work, the Navier-Stokes equations are solved numerically using the Nek5000 code developed by Fischer *et al.* (2008). The box of the DNS shall extend axially up to $z/D = 75$ to properly investigate not only the near-field but also the far-field behavior of self-preservation. In other round jet DNS like Boersma *et al.* (1998), Babu & Mahesh (2004) and Taub *et al.* (2013), top-hat profiles with small disturbances have been used. However, the transition to turbulence of the jet usually takes around $10D$ downstream of the orifice. That is why in the present DNS a turbulent pipe is used as an inlet condition to properly capture physics, which to the author's knowledge has not yet been reported to study round jets in the context of self-similarity.

It might have been in Oberlack (2001), where symmetries have been used in turbulence for the first time to generate invariant solutions, which in this context is equivalent to turbulent scaling laws. However, this approach was limited to the mean velocity, meaning the statistical moment of first order, at that time. This has been extended with Oberlack & Rosteck (2010), where they recognized that the MPMEs admit Lie symmetries that do not appear in either the Euler or the Navier-Stokes equations and are therefore called statistical symmetries. Usually, when dealing with turbulence statistics the Reynolds decomposition $U_i = \overline{U}_i + u_i$ is used where $\overline{U}_i$ denotes the mean velocity and u_i the turbulent fluctuations. In the Reynolds-averaged Navier-Stokes (RANS) model the instantaneous moment $\overline{U_i U_j}$ is decomposed into $\overline{U}_i\overline{U}_j + \overline{u_i u_j}$ where $\overline{u_i u_j}$ is called the Reynolds stress tensor. However, focusing on the MPMEs based on the instantaneous velocities, an infinite set of linear equations are received where the coupling between the equations is only between "neighboring" equations. By introducing $H_{ij} = \overline{U_i U_j}$ and $R_{ij} = \overline{u_i u_j}$, the omission of the Reynolds decomposition shall be called the H-approach and the classical approach is called the R-approach. Additionally, the instantaneous moments of an arbitrary order n can be introduced with $H_{i\{n\}}$ and the correlation at one point with $H^0_{i\{n\}} = \overline{U_i^n}$. By finding symmetries of the MPMEs, invariant solutions and therefore turbulent scaling laws can be derived rigorously. In the work of Sadeghi *et al.* (2018) and Sadeghi *et al.* (2021), this method has been used successfully for temporally evolving turbulent plane jets for not only velocity moments but also passive scalar moments. In addition to that, just recently in Hoyas *et al.* (2022) and Oberlack *et al.* (2022), they were able to derive turbulent scaling laws with this method for moments of arbitrary order in two regions of a turbulent channel flow and validated them with a new DNS of a Poiseuille channel flow at a friction Reynolds number of 10000.

Governing equations

The governing equations in this work are the Navier-Stokes equations for an incompressible flow consisting of the continuity equation

$$\nabla \cdot \mathbf{U} = 0 \tag{1}$$

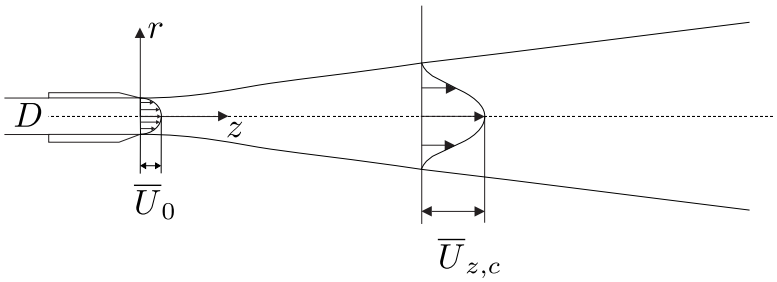

Figure 1: Schematic view of a round jet flow. Fluid is blown through a nozzle with diameter D. The mean axial centerline velocity at the orifice is denoted by $\overline{U}_0$ and the axial centerline velocity of the jet is denoted by $\overline{U}_{z,c}$

and the momentum balance equations

$$\frac{\partial \mathbf{U}}{\partial t} + (\mathbf{U}\cdot\nabla)\,\mathbf{U} = -\nabla P + \frac{1}{Re_0}\nabla^2\mathbf{U}. \tag{2}$$

with $\mathbf{U}$, P, $\mathbf{x}$, t being respectively velocity vector, pressure, the spatial coordinate and time. Further, the Reynolds number is defined as $Re_0 = U_0 D/\nu$ with D and U_0 being a length and velocity scale to be defined below.

DNS of the turbulent jet flow

The Navier-Stokes equations (1) and (2) are solved numerically using Nek5000 developed by Fischer *et al.* (2008). Nek5000 is a computational fluid dynamics solver based on spectral element method (SEM), which is a subclass of the weighted residuals method and therefore part of the Galerkin schemes. A thorough description of the numerical method can be found e.g. in Patera (1984). It uses a weak formulation of the Navier-Stokes equations and is solved on a hexahedral element mesh. SEM uses piecewise high-order Lagrange polynomials as basis functions similar to the finite element method. To integrate over each element, the Gauss-Lobatto-Legendre (GLL) integration is used. Besides accuracy, one of the main reasons for using Nek5000 in this work is the very efficient parallel implementation needed for the large scale DNS conducted. For optimal efficiency the polynomial order $N = 7$ is used as suggested by Fischer *et al.* (2008). Further, the BDF2 scheme has been used as a timestepping method. The adaptive timestep is controlled by the Courant number.

Computational domain of the DNS

Previous round jet DNS such as of Boersma *et al.* (1998), Babu & Mahesh (2004) and Taub *et al.* (2013) have employed top-hat profiles extended by small velocity disturbances as inlet profiles. The transition to a fully turbulent behavior of these jet usually take around $10D$ downstream of the inlet. For this reason in the present DNS we use a fully developed turbulent pipe as an inlet condition. Self-similarity is predicted to occur closer to the inlet and secondly, the inlet condition is physically more realistic. To accomplish that, the simulation has been split into two domains. One is that of a periodic pipe flow to generate the inlet condition and the other is the main computational domain to capture the turbulent jet flow.

The presently employed bulk Reynolds number has been chosen to be $Re_0 = 3500$. The bulk Reynolds number is defined as follows

$$Re_0 = \frac{U_{\text{bulk}} D}{\nu} \tag{3}$$

where U_{bulk} refers to the bulk average velocity at the inlet in streamwise direction, D to the pipe diameter and therefore also to the diameter of the inlet nozzle and ν to the viscosity. $Re_0 = 3500$ has been chosen to lie in a range of a fully turbulent pipe flow and still being computationally feasible with the available computational resources. The cross-section of the mesh contains 33 cells. Further, the mesh has 30 cells in axial direction and extends in that direction for $5D$. Factoring in the $N = 7$ GLL points, the pipe mesh has around 2 million grid points. Therefore we have a $1D \times 5D$ (diameter $\times$ axial length) mesh. The boundary conditions at the wall are no-slip and impermeable wall while at $z = -5D$ and $z = 0$ periodicity has been employed.
To generate a turbulent velocity field in the pipe a small disturbance in all three direction is added to the initial condition of a laminar pipe profile

$$U_z = 6(r^2 - R^2), \text{ with } R = 0.5. \tag{4}$$

Pressure gradient and viscosity are set, such that the bulk velocity is 1 and $Re_0 = 3500$. After running the simulation until a fully developed turbulent pipe flow has been reached, the velocities at the cross section $z = 0$ are interpolated onto the inlet of the main computational domain at each timestep. The main computational domain is a truncated cone with the axial length $75D$. At the inlet $z/D = 0$ the diameter is $4D$ and at the outlet $z/D = 75$ the diameter is $64D$. This ensures that the box is large enough to capture the spreading of the jet and that there is no interaction with the lateral far-field boundaries. The main computational mesh consists of two parts: The inner part contains the domain of a pipe and the outer part is a symmetrical cylindrical mesh which are scaled linearly in radial direction when moving axially. In axial direction the cells of both the pipe and the outer part are stretched geometrically with the factor of 1.006 with 234 cells. Around the inner part, the cells are stretched geometrically in transverse direction with the factor of 1.06 with 25 cells. Considering the $N = 7$ GLL points, the main computational mesh has around 180 thousand cells which amounts to 240 million degrees of freedom (DOFs). During the simulation, the periodic pipe at $z = 0$ is then interpolated onto the main computational domain at $z = 0$ so that a fully turbulent pipe inflow is achieved for the jet. Figure 2 shows isosurfaces of the q-criterion of the conducted jet flow.

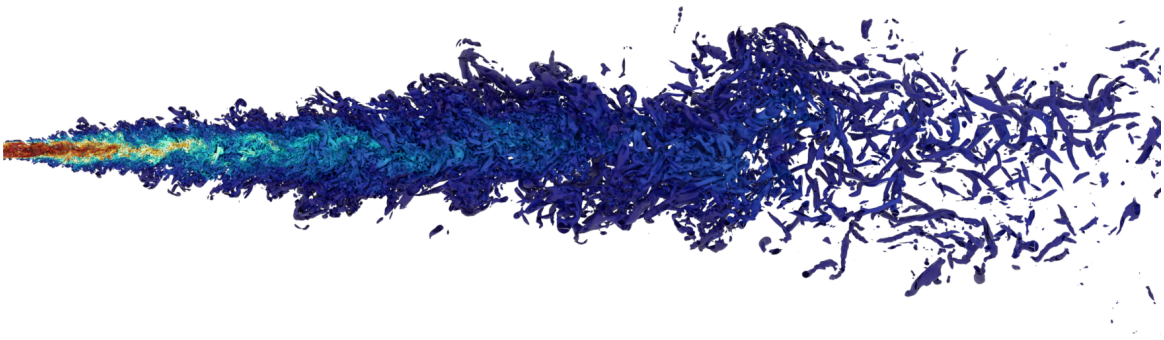

Figure 2: A cross section of q-criterion isosurfaces of the conducted jet DNS colored with the velocity magnitude ranging from 1.5 (red) to 0 (blue).

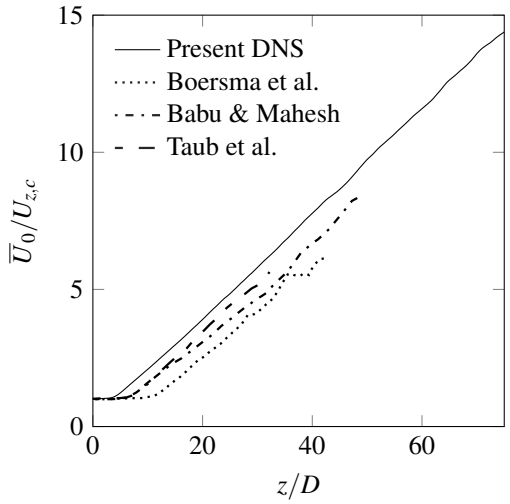

Figure 3: Inverse mean axial centerline velocity plotted over the distance from the orifice. The present DNS at $Re_0 = 3500$ is compared to various other DNS and experiments.

Classical scaling laws

In classical theory the mean velocities of a self-preserving jet are scaled with the centerline velocity

$$\frac{U_{z,c}(z)}{\overline{U}_0} = \frac{B_u D}{z - z_0}, \tag{5}$$

where $\overline{U}_0$ refers to the mean axial centerline velocity at the orifice, B_u to the decay constant and z_0 to the virtual origin. The inverse of the mean axial centerline velocity compared to other DNS and experiments can be depicted in Figure 3. Qualitatively, it can already be observed that the present DNS begins decaying earlier than any experiment conducted before. In Table 1 the parameters of the present DNS and other experiments are linked. It can be seen that the decay rate of the present DNS is slightly lower compared to the other experiments conducted. Additionally, the virtual origin lies behind the inlet which is due to early mixing because of the turbulent inlet.

Table 1: Parameters of the mean axial centerline velocity compared to other experiments.

Reference	Re_0	B_u	z_0
Boersma *et al.* (1998)	2400	5.9	4.9
Taub *et al.* (2013)	2000	5.4	1.3
Present	3500	5.29	−1.3

Symmetry based scaling laws

The symmetries needed for the derivation of the scaling laws are derived from the Euler equations and can be transferred to the MPMEs with the limit of $Re_0 \to \infty$. The MPMEs are derived by multiplying equation (2) with $n-1$ velocities at $n-1$ different locations $\mathbf{x}_i$ with a subsequent statistical averaging. This results in the MPMEs with order n

$$\frac{\partial H_{i_{\{n\}}}}{\partial t} + \sum_{l=1}^{n} \left[\frac{\partial H_{i_{\{n+1\}}[i_{(n)} \mapsto k_{(n)}]} \left[\mathbf{x}_{(n)} \mapsto \mathbf{x}_{(l)} \right]}{\partial x_{k_{(l)}}} + \frac{\partial I_{i_{\{n-1\}}[l]}}{\partial x_{i_{(l)}}} - \frac{1}{Re_0} \frac{\partial^2 H_{i_{\{n\}}}}{\partial x_{k_{(l)}} \partial x_{k_{(l)}}} \right] = 0 \tag{6}$$

where

$$H_{i_{\{n\}}} = \overline{U_{i_{(1)}}(\mathbf{x}_{(1)}) \cdot \ldots \cdot U_{i_{(i)}}(\mathbf{x}_{(i)})} \tag{7}$$

and $I_{i_{\{n-1\}}[l]}$ includes the correlations with the pressure. A deeper insight into MPMEs can be gained in Oberlack & Rosteck (2010).
In the present work, the focus is set on three symmetries. The first symmetry is a translation in space

$$\overline{T}_x: \quad t^* = t, \quad x_i^* = x_i + a_{x_i}, \quad r_i^* = r_i, \quad \overline{U_i}^* = \overline{U_i}, \quad H^*_{i_{\{n\}}} = H_{i_{\{n\}}} \tag{8}$$

and the second symmetry is a scaling in space and time

$$\begin{aligned}\overline{T}_t: \quad & t^* = \exp(a_{St})t, \quad x_i^* = \exp(a_{Sx})x_i, \quad r_i^* = \exp(a_{Sx})r_i, \\ & \overline{U_i}^* = \exp(a_{Sx}-a_{St})\overline{U_i}, \quad H^*_{i_{\{n\}}} = \exp(n(a_{Sx}-a_{St}))H_{i_{\{n\}}}, \\ & P^* = \exp(2(a_{Sx}-a_{St}))P. \end{aligned} \tag{9}$$

The third symmetry is a statistical symmetry, emerging from the linearity of the MPMEs reading as

$$\begin{aligned}\overline{T}_s: \quad & t^* = t, \quad x_i^* = x_i, \quad r_i^* = r_i, \quad \overline{U_i}^* = \exp(a_{Ss})\overline{U_i}, \\ & H^*_{i_{\{n\}}} = \exp(a_{Ss})H_{i_{\{n\}}}. \end{aligned} \tag{10}$$

The symmetries in equation (8)-(10) form the characteristic condition for a spatially developing turbulent round jet where subsequently we only consider one-point statistics, i.e. $\overline{U_i^n}$. Since a spatially round jet is symmetrical in azimuthal direction the characteristic condition gives

$$\begin{aligned}&\frac{\mathrm{d}z}{a_{Sx}z+a_z} = \frac{\mathrm{d}r}{a_{Sx}r} = \frac{\mathrm{d}\overline{U_iU_j}}{[2(a_{Sx}-a_{St})+a_{Ss}]\overline{U_iU_j}} \\ &= \frac{\mathrm{d}\overline{U_i}}{[a_{Sx}-a_{St}+a_{Ss}]\overline{U_i}} = ... = \frac{\mathrm{d}\overline{U_i^n}}{[n(a_{Sx}-a_{St})+a_{Ss}]\overline{U_i^n}}. \end{aligned} \tag{11}$$

By integrating equation (11) the following scaling laws can be derived:

$$\eta = \frac{r}{z+z_0} \tag{12a}$$

$$\widetilde{\overline{U}}_i(\eta) = \frac{\overline{U}_i(r,z)}{(z+z_0)^{-\lambda_1}} \tag{12b}$$

$$\widetilde{\overline{U_i^2}}(\eta) = \frac{\overline{U_i^2}(r,z)}{(z+z_0)^{-\lambda_2}} \tag{12c}$$

$$\widetilde{\overline{U_i^n}}(\eta) = \frac{\overline{U_i^n}(r,z)}{(z+z_0)^{n(\lambda_1-\lambda_2)-2\lambda_1+\lambda_2}} \tag{12d}$$

where

$$z_0 = \frac{a_z}{a_{Sx}}, \quad \lambda_1 = \frac{a_{St}}{a_{Sx}} - \frac{a_{Ss}}{a_{Sx}} - 1, \quad \lambda_2 = 2\frac{a_{St}}{a_{Sx}} - \frac{a_{Ss}}{a_{Sx}} - 2. \tag{13}$$

The constant n refers to the order of the velocity moments. If $n=1$ or $n=2$ are respectively introduced into (12d), the mean velocity scaling in equation (12b) or the second order velocity moments in equation (12c) are obtained. The free parameters λ_1 and λ_2 are the exponents of the first and second velocity moment. The self-preservation of three axial moments can be seen in Figure 4.

Validation of the symmetry based scaling laws

In order to validate the symmetry-induced scaling laws of the velocities we set $r=0$ and the equation (12d) needs to be rearranged to

$$\overline{U_i^n}(r=0,z) = \frac{C_{i,n}}{(z+z_0)^{n(\lambda_2-\lambda_1)+2\lambda_1-\lambda_2}}, \text{ for } n \geq 1 \;\&\; i = r,\varphi,z, \tag{14}$$

Table 2: Parameters of equation (15) for each direction r, φ, z.

i	$\alpha_{u,i}$	$\beta_{u,i}$
r	0.135	1.273
φ	0.133	1.270
z	0.683	2.284

where $\widetilde{\overline{U_i^n}}(\eta=0) = \widetilde{\overline{U_{i,c}^n}} = C_{i,n}$. The virtual origin $z_0 = 1.276$ can be determined by the spreading rate of the first moment while $\lambda_1 = 1.036$ and $\lambda_2 = 2.068$ can be received by fitting the axial centerline to the first and second moment in z-direction. All higher moments determine $C_{i,n}$ which show the relation as seen in Figure 5. These constants follow the relation

$$C_{i,n} = \alpha_{u,i}\mathrm{e}^{n\beta_{u,i}}, \tag{15}$$

quite accurately with $R^2 = 0.99$ for all fits. The constants for the r and φ-direction only differ by around 1.5% as seen in Table 2 which is due to symmetry. In conclusion, this means that the scaling of all moments of arbitrary order can be determined with

$$\overline{U_i^n}(r=0,z) = \frac{\alpha_{u,i}\mathrm{e}^{\beta_{u,i}n}}{(z+z_0)^{n(\lambda_2-\lambda_1)+2\lambda_1-\lambda_2}}. \tag{16}$$

Radial scaling of a turbulent round jet

There have been many works e.g. Panchapakesan & Lumley (1993), noticing that the radial profile of the mean axial velocity (see Figure 4) behaves similar to a Gauss-type profile. However, we have yet to understand where this behavior comes from and if this can be derived from the underlying equations. Comparing the radial profiles of the higher instantaneous axial moments leads to the conclusion that also the scaled higher axial moments in (12) can be fitted to a Gaussian which leads to

$$\frac{\widetilde{\overline{U_z^n}}(\eta)}{\widetilde{\overline{U_{z,c}^n}}} = \mathrm{e}^{-\gamma_n\eta^2}, \tag{17}$$

where, when comparing with (12), (15) and (16), we have $\widetilde{\overline{U_{z,c}^n}} = C_{z,n} = \alpha_{u,z}\mathrm{e}^{n\beta_{u,z}}$. The DNS data up to the tenth axial moment are presented in Figure 6 where, due to a logarithmic scaling, a parabolic exponent of the moments suggests that equation (17) fits quite well. A very good linear fitting in n of γ_n for the axial moments can be taken from Figure 7.
Equation (2) in z-direction can be statistically averaged in its conservative form and taking the limit of $Re_0 \to \infty$ gives

$$\frac{\partial\overline{U_rU_z}}{\partial r} + \frac{\partial\overline{U_z^2}}{\partial z} = 0. \tag{18}$$

If then, equations (12) and (17) are implemented in equation (18) for $n=2$ and also using a similar scaling law for $\overline{U_rU_z}$ we obtain $\widetilde{\overline{U_rU_z}}(\eta) = \overline{U_rU_z}(r,z)/(z+z_0)^{-\lambda_2}$, and finally receive

$$\widetilde{\overline{U_rU_z}} + \eta\frac{\partial\widetilde{\overline{U_rU_z}}}{\partial\eta} = C_1\eta\left(\lambda_2 - 2\gamma_2\eta^2\right)\mathrm{e}^{-\gamma_2\eta^2}, \tag{19}$$

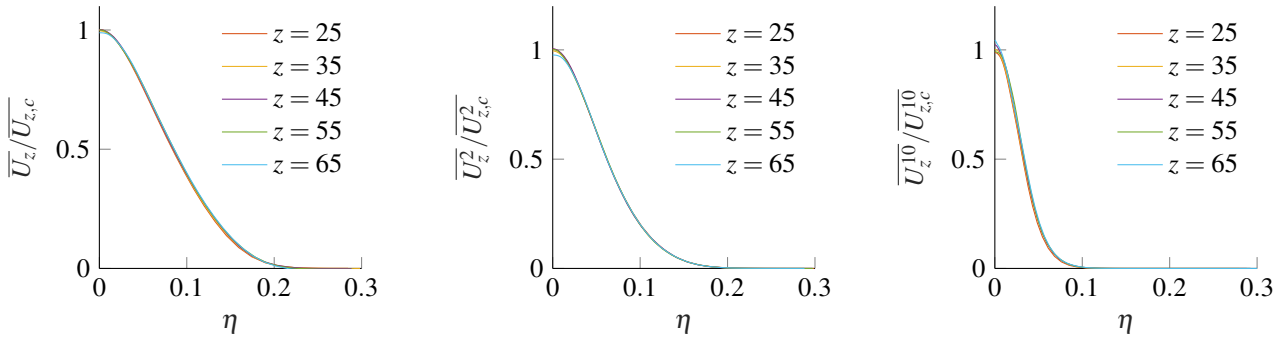

Figure 4: The radial profiles of the (a) 1st, (b) 2nd and (c) 10th axial moment normalized with the scalings in (12).

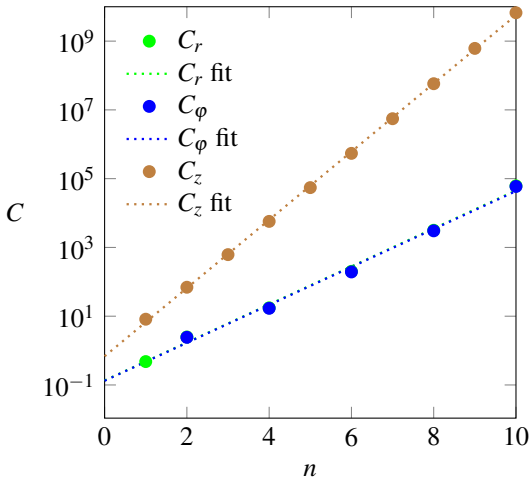

Figure 5: Constants $C_{i,n}$ according to the equation (15) are shown for each moment up to order $n = 10$ for each direction and determined by fitting to the DNS.

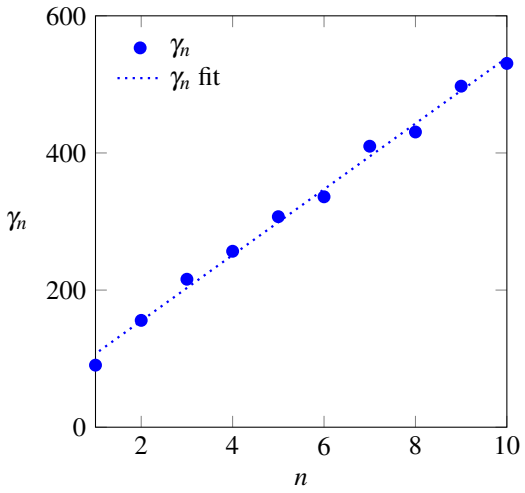

Figure 7: Constants γ_n from equation (17) are shown for each moment up to order $n = 10$ determined by fitting to the DNS yielding the following fit: $\gamma_n = 48.0n + 59.2$.

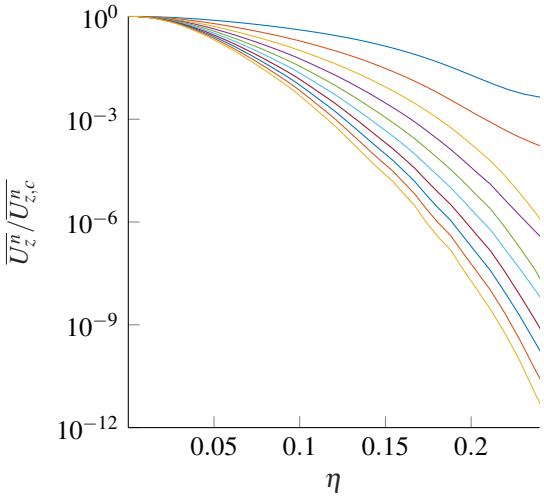

Figure 6: The radial profiles of the 1st (top) up to the 10th (bottom) axial moment, normalized with the scaling in equation (12) and shown in a semi-logarithmic plot at $z = 45$.

leading to the solution

$$\widetilde{\overline{U_r U_z}}(\eta) = \frac{\widetilde{\overline{U_{z,c}^2}}}{2\gamma_2\eta}\left[\left(2\gamma_2\eta^2 - \lambda_2 + 2\right)\mathrm{e}^{-\gamma_2\eta^2} + (\lambda_2 - 2)\right], \tag{20}$$

where $C_1 = \widetilde{\overline{U_{z,c}^2}}$ and the integration constant $C_2 = [C_1(\lambda_2 - 2)]/(2\gamma_2)$ have been derived from the boundary condition $\lim_{\eta\to 0}\widetilde{\overline{U_r U_z}}(\eta) = 0$. Plotting the solution and the DNS data of $\overline{U_r U_z}$ in Figure 8 one can see, that they behave similarly. Following up on this, that could mean that there is another statistical symmetry hidden in the MPMEs that we have yet to find analytically and which could explain the Gaussian behavior of the axial moments.

Conclusion and Outlook

A DNS of a spatially evolving turbulent round jet has been conducted with a turbulent pipe flow as an inlet at $Re_0 = 3500$. Contrary to works in the past, a turbulent pipe flow with $Re_0 = 3500$ has been used as an inlet to shorten the transition region. Further, new scaling laws for a spatially turbulent

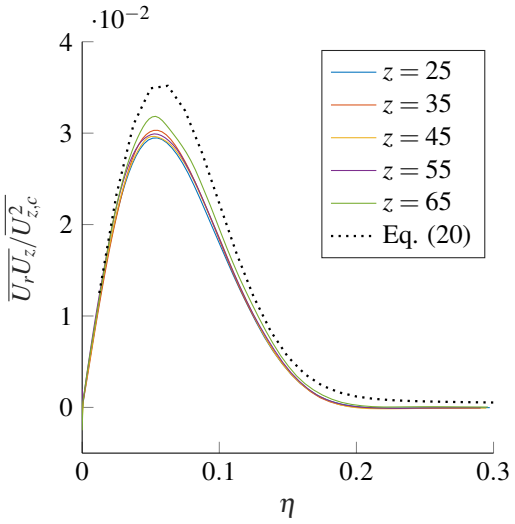

Figure 8: The radial profiles of $\overline{U_r U_z}$ at different distances z from the orifice compared to the solution in equation (20).

round jet have been derived for the velocity using Lie symmetry analysis. The scaling laws are then validated by the DNS. It has been shown that, the velocity moments are dependent of 7 different parameters. By determining the parameters using the DNS, all moments up to an arbitrary order are determined by the scaling laws.

Similarly to previous work, the radial moment scaling has been fitted to a Gaussian distribution. This also works very well for the higher moments where a linear behavior of the constant in the exponent has been detected. With the assumption of a Gaussian radial scaling and the invariants derived using Lie symmetry analysis, the radial scaling of $\overline{U_r U_z}$ has been derived which behaves similarly to the DNS data.

The next steps would be to conduct additional DNS with a higher Reynolds number, at different co-flow rates and different inlet conditions (e.g. synthetic jets) to investigate how the free parameters of the symmetry based scaling laws are influenced. For that, DNS data is needed which can be generated by modifying the current DNS setup. Also, the analysis of the radial scaling might suggest the existence of an additional statistical symmetry that can explain the Gaussian distribution. Therefore, a deeper analysis of the MPMEs should be undertaken regarding the existence of additional symmetries. Additionally, as all symmetries of the moment equations have their counterpart in the Lundgren-Novikov-Monin probability density function (PDF) approach, we can also construct turbulent scaling laws for the PDF functions. Here, it is intended to construct symmetry invariant PDF up to its two-point version and compare this to the PDF generated from the DNS data.

REFERENCES

Babu, P. C. & Mahesh, K. 2004 Upstream entrainment in numerical simulations of spatially evolving round jets. *Physics of Fluids* **16** (10), 3699–3705.

Boersma, B. J., Brethouwer, G. & Nieuwstadt, F. T. M. 1998 A numerical investigation on the effect of the inflow conditions on the self-similar region of a round jet. *Physics of Fluids* **10** (4), 899–909.

Fischer, P. F., Lottes, J. W. & Kerkemeier, S. G. 2008 nek5000 web page.

Hoyas, Sergio, Oberlack, Martin, Alcántara-Ávila, Francisco, Kraheberger, Stefanie V. & Laux, Jonathan 2022 Wall turbulence at high friction reynolds numbers. *Phys. Rev. Fluids* **7** (1), 014602.

Oberlack, Martin 2001 A unified approach for symmetries in plane parallel turbulent shear flows. *J. Fluid Mech.* **427**, 299–328.

Oberlack, Martin, Hoyas, Sergio, Kraheberger, Stefanie V., Alcántara-Ávila, Francisco & Laux, Jonathan 2022 Turbulence statistics of arbitrary moments of wall-bounded shear flows: A symmetry approach. *Phys. Rev. Lett.* **128** (2), 024502.

Oberlack, Martin & Rosteck, Andreas 2010 New statistical symmetries of the multi-point equations and its importance for turbulent scaling laws. *Discrete & Continuous Dynamical Systems - S* **3** (3), 451–471.

Panchapakesan, N. R. & Lumley, J. L. 1993 Turbulence measurements in axisymmetric jets of air and helium. part 1. air jet. *0022-1120* **246**, 197–223.

Patera, A. T. 1984 A spectral element method for fluid dynamics: Laminar flow in a channel expansion. *Journal of Computational Physics* **54** (3), 468–488.

Sadeghi, H., Oberlack, M. & Gauding, M. 2018 On new scaling laws in a temporally evolving turbulent plane jet using lie symmetry analysis and direct numerical simulation. *0022-1120* **854**, 233–260.

Sadeghi, H., Oberlack, M. & Gauding, M. 2021 New symmetry-induced scaling laws of passive scalar transport in turbulent plane jets. *0022-1120* **919**.

Taub, G. N., Lee, Hyungoo, Balachandar, S. & Sherif, S. A. 2013 A direct numerical simulation study of higher order statistics in a turbulent round jet. *Physics of Fluids* **25** (11), 115102.